HHS Public Access

Author manuscript

Cellulose (Lond). Author manuscript; available in PMC 2016 July 25.

Published in final edited form as:

Cellulose (Lond). 2016 June ; 23(3): 1763–1775. doi:10.1007/s10570-016-0947-5.

Impacts of chemical modification on the toxicity of diverse nanocellulose materials to developing zebrafish

Bryan J. Harper,
Department of Environmental and Molecular Toxicology, Oregon State University, 1007 ALS Building, Corvallis, OR 97331, USA

Alicea Clendaniel,
Department of Environmental and Molecular Toxicology, Oregon State University, 1007 ALS Building, Corvallis, OR 97331, USA

Federico Sinche,
Department of Environmental and Molecular Toxicology, Oregon State University, 1007 ALS Building, Corvallis, OR 97331, USA

Daniel Way,
Department of Wood Science and Engineering, Oregon State University, Corvallis, OR, USA

Michael Hughes,
Department of Wood Science and Engineering, Oregon State University, Corvallis, OR, USA

Jenna Schardt,
Department of Wood Science and Engineering, Oregon State University, Corvallis, OR, USA

John Simonsen,
Department of Wood Science and Engineering, Oregon State University, Corvallis, OR, USA

Aleksandr B. Stefaniak, and
National Institute for Occupational Safety and Health, Morgantown, WV, USA

Stacey L. Harper
Department of Environmental and Molecular Toxicology, Oregon State University, 1007 ALS Building, Corvallis, OR 97331, USA

School of Chemical, Biological and Environmental Engineering, Oregon State University, Corvallis, OR, USA

Oregon Nanoscience and Microtechnologies Institute (ONAMI), Corvallis, OR, USA

Stacey L. Harper: stacey.harper@oregonstate.edu

Abstract

Correspondence to: Stacey L. Harper, stacey.harper@oregonstate.edu.

Compliance with ethical standards

Ethical approval All appropriate international, national and/or institutional guidelines for the care and use of animals were followed.

Conflict of interest The authors declare that they have no conflict of interest.

Cellulose is an abundant and renewable resource currently being investigated for utility in nanomaterial form for various promising applications ranging from medical and pharmaceutical uses to mechanical reinforcement and biofuels. The utility of nanocellulose and wide implementation ensures increasing exposure to humans and the environment as nanocellulose-based technologies advance. Here, we investigate how differences in aspect ratio and changes to surface chemistry, as well as synthesis methods, influence the biocompatibility of nanocellulose materials using the embryonic zebrafish. Investigations into the toxicity of neutral, cationic and anionic surface functionalities revealed that surface chemistry had a minimal influence on the overall toxicity of nanocellulose materials. Higher aspect ratio cellulose nanofibers produced by mechanical homogenization were, in some cases, more toxic than other cellulose-based nanofibers or nanocrystals produced by chemical synthesis methods. Using fluorescently labeled nanocellulose we were able to show that nanocellulose uptake did occur in embryonic zebrafish during development. We conclude that the benign nature of nanocellulose materials makes them an ideal platform to systematically investigate the inherent surface features driving nanomaterial toxicity in order to create safer design principles for engineered nanoparticles.

Keywords

Nanocellulose; Zebrafish; Surface chemistry; Nanofibers; Nanocrystals

Introduction

Nanocelluloses, including cellulose nanocrystals (CNCs) and cellulose nanofibers (CNFs), are highly desired because they can be obtained from numerous renewable resources such as wood, cotton, linen, paper, algae and bacteria (Hanif et al. 2014; Moon et al. 2011). Both nanocrystalline and nanofibrous forms of cellulose materials are generating great interest due to their high chemical stability, physicochemical properties, commercial importance, and the ease with which these nanoparticles can be modified both structurally and chemically (Jackson et al. 2011; Lam et al. 2012a, b; Peng et al. 2011). Nanocellulose and its derivatives are currently exploited in applications such as mechanical reinforcement, bioimaging, catalysis, enzyme immobilization and drug delivery (Dufresne 2013; Jackson et al. 2011; Lam et al. 2012a, b; Moon et al. 2011; Peng et al. 2011). Most, if not all, of these applications will lead to large-scale production of nano-sized cellulose materials and inevitably an increased risk of exposure for humans and the environment. Given the myriad of potential uses for such biopolymers, there is a need to investigate how potential structural and chemical alterations to nanocellulose can impact its biocompatibility.

Past toxicological studies of nanocellulose materials have focused primarily on cytological or inhalation toxicity of parent materials, and very limited data is available on vertebrate toxicity or the impact of surface chemical modifications (Roman 2015). In the present study, we examine the relative influence that aspect ratio, chemical and mechanical methods of synthesis and surface functionalization with various chemical moieties have on the toxicity of the predominantly benign parent cellulose materials. Studying the differential toxicity will provide insight into how to design efficient nanocellulose materials that impart minimal

hazard. Findings from this work will also elucidate the role of inherent features of nanoparticles, such as size and surface charge, have on overall nanoparticle biocompatibility.

The structural geometry of CNCs and CNFs is typically a rigid elongated or rod-like particle with widths ranging from 5 to 70 nm and lengths between 100 nm and several micrometers, depending on the origin source and extraction process (Brinchi et al. 2013; Elazzouzi-Hafraoui et al. 2007; Siqueira et al. 2010). The nanometric dimensions of CNCs and the high degree of molecular order result in physicomechanical properties that include high surface area-to-volume ratio, large aspect ratio (typically 20–70), high strength, high stiffness and thermal stability up to ~200 °C (Dufresne 2013; Isogai et al. 2011; Moon et al. 2011). CNCs and CNFs are generated through a combination of chemical and mechanical methods. In general, the process starts with the liberation of cellulosic fibers from natural biomaterials such as wood, cotton, linen, tunicate, etc. (Moon et al. 2011). Specific chemical and mechanical synthesis methods to extract the nanocellulose include acid hydrolysis, 2,2,6,6-tetramethylpiperidine-1-oxyl radical (TEMPO) mediated oxidation, enzyme pretreatment and mechanical homogenization (Eichhorn et al. 2010; Gousse et al. 2002; Stelte and Sanadi 2009; Turbak et al. 1983).

Acid hydrolysis is the main chemical process used to extract CNCs, which consists of exposing cellulose fibers to harsh acid treatment to release individual crystalline regions (Isogai et al. 2011). CNFs can be extracted from biomass by TEMPO-mediated oxidation of native cellulose to nanoscale fibers. Carboxylation that occurs along the surface facilitates further chemical modification, while also increasing aqueous dispersibility due to the electrostatic stabilization provided by the negatively charged carboxyl groups (Moon et al. 2011; Stelte and Sanadi 2009). Other methods of obtaining CNF (also called microfibrillated cellulose or MFC) include mechanical methods such as steam explosion, high-pressure homogenization and high speed shear or grinding (Dufresne 2013; Moon et al. 2011). In general, the nanosized fibrils are extracted from the native celluloses by enzymatic pretreatment followed by mechanical processing and/or homogenization in water using a supermasscolloider grinder, high shear refiner or a high-pressure homogenizer to yield particles with lengths up to several micrometers and widths typically in the 25–100 nm range (Goussé et al. 2002; Morandi et al. 2009; Turbak et al. 1983). Mechanical methods can be followed by chemical treatments to remove non-fibrillated fractions or to chemically functionalize the particle surface (Dufresne 2013; Goussé et al. 2002; Moon et al. 2011; Morandi et al. 2009).

Surface chemical modification of nanocellulose materials is an emerging alternative for the fabrication of new nanostructures due to its generally benign nature in bulk form (Azizi Samir et al. 2005; Brinchi et al. 2013). Chemical modifications of CNCs that have been reported include esterification, cationization, carboxylation, silylation and polymer grafting (Moon et al. 2011; Morandi et al. 2009; Müller et al. 2014; Stelte and Sanadi 2009). Most of these techniques use the abundance of hydroxyl groups on the surface to facilitate the easy conjugation of desired molecules (Eichhorn et al. 2010; Peng et al. 2011; Sharifi et al. 2012). While these chemical modifications have focused on the improvement of material dispersibility and compatibility, there are limited data regarding the toxic potential of such modifications to CNCs (Alexandrescu et al. 2013; Hua et al. 2014). Considering the effect of

surface chemistry on the biological response of other types of nanomaterials, it is imperative to understand the interactions between surface-modified cellulose materials and biological systems (Fubini et al. 2010).

Our objective was to determine the relative influence that aspect ratio and surface chemical modifications (which alter the surface charge of nanocellulose materials) have on the behavior and toxicity of nanocellulose materials in a complex biological system. Using embryonic zebrafish (*Danio rerio*) as a vertebrate model of toxicity, we examined the behavioral and morphological impacts elicited from exposure to various CNC materials (Table 1). To achieve this objective, the surface chemistry of CNCs were chemically modified to incorporate anionic, cationic and neutral (non-ionic) functional groups. In addition, we investigated the impact of mechanical and chemical synthesis methods on the toxicity of two wood-based CNF materials. Our goal was to identify inherent nanocellulose features that can be used to predict biological fate and toxicity; thus providing information suitable for the development of safer design rules for the continued development of biocompatible applications of sustainable nanocellulose-based materials.

Experimental

Cellulose nanocrystals (CNCs)

CNC stock concentrations ranged from 0.5 to 5.5 % solids and were sourced from cotton (ground Whatman #1 filter paper) or wood pulp (Table 1). The CNC-Carb was Nanocel (BioVision Enterprises Inc., New Minas, Nova Scotia, Canada) produced from wood pulp and the samples from the Forest Products Laboratory (CNC-Sulf, CNF-FPL-T, CNF-FPL-H) were from prehydrolysis kraft dissolving pulp. In addition, two different initial surface chemistries were established from cotton (sulfated CNC denoted as S.CNC and carboxylated CNC denoted as C.CNC) using established acid hydrolysis techniques (Peng et al. 2011) to provide the starting materials for further chemical modification.

Sulfated CNCs (S.CNC) were obtained by partial hydrolysis of ground cotton filter paper (Whatman 1) with 65 % H_2SO_4 (v/v) solution at 45 °C with medium stirring for 50 min. The ground paper to acid ratio was 1:10 g/mL. The mixture was centrifuged five times with reverse osmosis (RO) water prepared using Omnipure K series cartidges (Omnipure Filter Company, Caldwell, Idaho) to remove the spent acid. The suspension was then subjected to ultrasonic irradiation in a Branson Sonifier (Danbury, CT) for 15 min to disperse the CNCs and break any agglomerates formed. Sonication appeared to improve the dispersion as there were fewer settled solids after sonication and settling. The suspension was next dialyzed (10 kD cutoff) in RO water to remove salts until the conductivity was <100 μS/cm. Dispersed CNCs were then concentrated in a Rotavaporizer R1 10 (Buchi, Flawil, Switzerland) to obtain an aqueous dispersion of 1 % CNCs. The resulting sulfated CNCs were stored at 4 °C until further surface chemical modifications were performed.

Cationic surface modification was conducted by conjugating a quarternary ammonium species (glycidyltrimethylammonium chloride, GMAC) to the hydroxyl groups of stock S.CNC materials according to previously published methods (Hasani et al. 2008). The resulting solution was filtered through 25 μm filter paper (Whatman #4) to collect the CNCs

and dialyzed with RO water for 48 h until the conductivity dropped to 4.6 μS/mL, producing a stock CNC-GMAC suspension at a concentration of 0.43 % solids by weight.

Carboxylated nanocrystals for further chemical modification (C.CNC) were synthesized by combining ~ 50.00 g of ground cotton filter paper (Whatman 1) with 1 L of 2.4 M HCl in a 3 L 3-neck round bottom flask (RBF) equipped with a mixer, reflux condenser, and a glass needle adapter connected to an N_2 (g) source and heated (~ 100 °C) in an oil bath to reflux for 2 h under a steady stream of N_2 (g). It was then diluted with RO water, allowed to settle and the clear supernatant was removed by siphon without disturbing the pellet. The remaining solution was then stirred for about 10 min, then filtered through 25 μm filter paper (Whatman #4) to collect the cellulose cake, which was then rinsed with about 500 mL RO water. Once the pH exceeded 3, the dispersed cellulose particles were concentrated in a Rotavaporizer R110 (Buchi, Flawil, Switzerland) to obtain an aqueous dispersion of 1 % by weight agglomerated cellulose nanocrystals.

TEMPO carboxylation of the CNC material was then conducted by transferring 200 mL of the 1 % by weight cellulose suspension into a 3-neck RBF and slowly stirred with 140 mg of TEMPO (0.896 mmol), 360 mg of NaBr (3.498 mmol) and 10 mL of 11 % sodium hypochlorite (NaClO) with the aim of oxidation and conversion of the surface C6 primary hydroxyls to carboxylic acids. The reaction mixture was kept at a pH level of 10.2–10.5 for the entire reaction by adding NaOH (55–60 mL) automatically via a pH controller. After reacting for 4–8 h, 30–40 mL of ethanol was added to destroy the residual NaOCl and thereby terminate further oxidation. The mixture was purified by successively diluting with RO water and concentrating via diafiltration until a low conductivity (typically several hundred μS/cm) was reached (Isogai et al. 2011). The resulting carboxylated CNCs were stored at 4 °C until use.

The level of carboxylation was approximately 1 mmol/g CNC, while the sulfation was 0.2–0.3 mmol/g. The levels of surface carboxylation and sulfation were determined by performing a conductivity titration (Thermo Scientific conductivity meter equipped with Orion Probe #011050MD) using 0.01 M HCl and 0.01 N NaOH (Lasseuguette 2008). The carboxylated CNCs were used for further chemical modification with 2-,2-aminoethoxyethanol (AEE), ethylenediamine, hexamethylenediamine and taurine (2-aminoethanesulfonate) to obtain neutral and anionic charges respectively, according to established methods (Hemraz et al. 2013). CNC-Ethyl was synthesized from the CNC-Carb rather than the stock C.CNC.

To prepare Rhodamine B labeled CNC (CNC-Rhod) amine-grafted CNC was first synthesized by combining 124 g of TEMPO carboxylated cellulose nanocrystal (C.CNC) solution (0.81 % w/w, with 1.0 mmol carboxylation/g of cellulose) with 0.096 g (0.5 mmol) 1-Ethyl-3-[3-dimethylaminopropyl]carbodiimide hydrochloride (EDC) and 0.12 g (1 mmol) *N*-hydroxysulfosuccinimide (NHS) in 15 mL 0.1 M phosphate buffer (pH 6.5) and stirring for 1 h. A control was prepared using the same method, but without the EDC. 60 μL (1 mmol) of ethanolamine and 60 μL (1 mmol) ethylenediamine was added to the sample and control and was stirred for 1 h. Both the sample and control were quenched with 0.30 g (4.5 mmol) hydroxylamine hydrochloride and stirred for another 15 min. The samples were then

placed in dialysis tubing (Spectra/Por membrane, MWCO 12–14,000) and dialyzed for 3 days with the dialysis tank water replaced every 12 h.

Separately, a similar EDC reaction was performed on the hydroxyl group of the Rhodamine B by adding 0.24 g (0.5 mmol) Rhodamine B to 20 mL of 0.1 M phosphate buffer (pH 6.5) with 0.20 g (1 mmol) EDC and 0.23 g (2 mmol) of NHS and stirred for 1 h. Again, a control solution was made up in which EDC was omitted, but otherwise prepared using the same method. These solutions were added to their respective amine-grafted CNC solutions (prepared as described above) and stirred for 1 h. Both the sample and control were quenched with 0.30 g (4.5 mmol) hydroxylamine hydrochloride and stirred for 15 min. The samples were placed in dialysis Spectra/Por molecularporous membrane tubing (MWCO 12–14,000) and dialyzed for 14 days with tank water replaced every 12 h for the initial 3 days and then daily for the remainder. The final sample was 0.31 % by weight Rhodamine B labelled CNC.

Cellulose nanofibers (CNF)

CNF materials were provided by two sources, USDA Forest Products Laboratory, Madison, WI (under arrangements for testing with NIOSH) and the University of Maine Process Development Center, Orono, ME nanocellulose pilot plant. The Forest Products laboratory provided two types of CNFs. The first, designated CNF-T (concentrated to 0.84 % solids) was made by TEMPO-mediated oxidation of source cellulose which selectively carboxylates the carbon at position 6 of the glucose ring in cellulose molecules. The second material, referred to as CNF-H (concentrated to 0.5 % solids) made by mechanical homogenization which does not change the surface hydroxyl group chemistry. The University of Maine pilot plant provided CNF concentrated to 1.5 % solids, also made by mechanical homogenization using wood pulp as a starting material. All cellulose-based nanomaterials and their physicochemical characteristics are provided in Table 1.

Nanocellulose characterization

After the preparation of the CNC materials, each sample was evaluated using gravimetric analysis for % solids. Zeta potential (ζ) values were measured in the fishwater exposure solution (see exposure section below for details) at 50 mg/L using a Zetasizer Nano (Malvern Instruments Ltd, UK). Zeta potential measurements were conducted in triplicate using the Smoluchowski equation for electrophoretic mobility to calculate the mean and standard deviation. An FEI Titan 80–200 transmission electron microscope (TEM) was employed for primary particle size analysis. The grids used were Ted Pella PELCO Formvar 400 mesh copper grids. The grids were plasma charged in a Ted Pella PELCO easiGlow glow discharge instrument to achieve hydrophilicity. 2 μL drops of 0.01–0.05 % solids solution of the various samples were dropped onto grids and allowed to dry for 5 min. After 5 min the remaining solution was wicked off with a small strip of whatman filter paper. The samples were then stained with 2 μL of either 1 % sodium (K) phosphotungstate (PTA) or 2 % ammonium molybdate for 1 min until being wicked off again with whatman filter paper. The samples were imaged at imaged at 80 or 200 kV. The dimensions of a minimum of five particles were determined to calculate the average particle size of each material.

Zebrafish exposures

Fishwater for dilution of CNC suspensions was prepared by diluting 0.26 g/L Instant Ocean salts (Aquatic Ecosystems, Apopka, FL) into RO water and adjusting the pH to 7.2 ± 0.2 with sodium bicarbonate. Embryonic exposure solutions were prepared as dispersions in fishwater by first diluting each nanocellulose sample with fishwater to make a 2000 mg/L stock solution. The 2000 mg/L stock solution was then further diluted with fishwater to the final test concentrations of 0.2, 2.0, 20.0 and 200.0 mg/L for CNCs (except for CNC-GMAC which was tested at slightly differing concentrations of 0.3, 1.4, 6.8, 34.4 and 172 due to a revision in the percent solids analysis after dilution). The CNF samples were treated in the same fashion, using fishwater to dilute the samples to 2000 mg/L, then subsequently diluted with fishwater to the final test concentrations (2.0, 5.0, 10.0 and 250.0 mg/L). Following dilution with fishwater, exposure solutions were mixed gently for 2 min prior to starting the zebrafish exposures.

Zebrafish embryos (*D. rerio*, wild type, 5D-Tropical strain) were obtained from the Sinnhuber Aquatic Research Laboratory at Oregon State University. Embryos were staged such that the chorion surrounding the embryo could be removed enzymatically at 6 h post-fertilization (hpf) (Usenko et al. 2008). Dechorionation was performed to ensure direct contact of the materials with the developing embryo by exposing groups of 200–400 embryos to 1.5 mL of 50 mg/mL Protease from *Streptomyces griseus* (Sigma Aldrich, St. Louis, MO) in a 60 mm glass petri dish for approximately 6 min until the chorion begins to detach, then gently rinsing the embryos thoroughly with fishwater to complete the removal.

Embryos were exposed individually in clear 96-well plates filled with 200 μL of each cellulose-based nanomaterial suspension, such that each plate had 12 embryos exposed to each concentration of nanomaterial. At least two replicate plates were conducted for each material using different clutches of embryos, thus a minimum of 24 embryos were exposed to each concentration of nanomaterial. The plates were sealed with laboratory film and kept under a 14:10 h light:dark photoperiod at 26.8 °C for 5 days. Exposed embryos were evaluated at 24 hpf for viability, notochord malformations, developmental progression, and spontaneous movement; then at 120 hpf for behavioral endpoints (motility, tactile response), larval morphological abnormalities (body axis, eye, snout, jaw, otic vesicle, heart, brain, somite, fin, yolk sac, pigmentation, trunk), and physiological function (circulation, pigment, swim bladder). Endpoints were evaluated in vivo and scored in a binary fashion as either present or absent (Truong et al. 2011).

For uptake analysis, embryonic zebrafish were exposed to Rhodamine B labeled CNC using the same exposure paradigm previously discussed, except half of the embryos were exposed with their chorion intact in order to investigate the chorion's role in preventing CNC uptake. The amount of free Rhodamine was selected to match the concentration in the CNC-Rhod samples by standardizing the concentration colorometrically based on an excitation at 540 nm and emission measured at 625 nm. Embryos were removed from exposure solutions on days 1–5 of the exposure, rinsed 3 times with RO water and anesthetized for fluorescent imaging. Embryos from exposures where the chorion was left intact were manually removed from the chorionic membrane prior to imaging. The images were analyzed with ImageJ software to determine the relative intensity after embryo exposure to 0, 100 and 500 mg/L

Rhodamine B labeled CNC. All zebrafish exposures were conducted in accordance with all institutional and national guidelines.

Data analysis

Data from replicate 96-well plates were compared using analysis of variance (ANOVA) and replicate plates were pooled when no significant differences existed between replicate plates. Individual endpoint responses were assessed using the Fishers Exact test when the number of observations included in the data set was <100, and the Chi Square test when the number of observations was >100. The level of significance for statistical analysis was maintained at $p \leq 0.05$ for all analyses. Statistical comparisons were conducted using SigmaPlot version 12.2 (Systat Software, San Jose, CA, USA).

Results and discussion

Nanocellulose characterization

The physicochemical characterizations of the cellulose-based nanomaterials are listed in Table 2 including the length and width calculated from TEM images. Representative TEM images of test CNC materials can be found in Fig. 1. Overall there was little variation in longitudinal and transverse dimensions of CNC between the various types of CNC materials. The average length of the cellulose nanocrystals was 120 nm with an average width of 9 nm (Table 2). The elongated structure of the CNFs precluded measurement of fiber length through TEM.

The zeta potential (ζ) of each material in the exposure media, is representative of the interaction of the surface charge with the surrounding medium and is listed in Table 2. The cationic surface functionalization of CNC (CNC-GMAC) resulted in a mildly positive zeta potential, while all other materials showed negative zeta potential in the exposure media (Table 2). The relatively low zeta potential for the CNC-GMAC ($\zeta = 5.1$ mV) suggests that agglomeration of this particular sample was likely to occur to a greater extent than the other samples with much higher absolute values for their zeta potential (Riddick 1968). This agglomeration, in turn, can impact the bioavailability of the CNCs to the developing fish; however, in our experiments the fish were contained in wells with the suspensions, thus any agglomeration and settling would only serve to increase the effective exposure to the embryos laying on the bottom of each well. The high absolute value of the zeta potential for the CNC materials with anionic ligands suggests good stability in the colloidal suspensions (Riddick 1968). The addition of the neutrally charged ligands only resulted in a slight reduction in the −46.7 mV potential of the C.CNC starting material in CNC-AEE and CNC-Hex (−26.9 and −29.0, respectively). In addition, a similar slight reduction in zeta potential was observed following quaternization of the CNC-Carb to CNC-Ethyl (Table 2). These ligands presented synthetic difficulties in conferring positive charges via quaternization, as increased levels of ligand binding led to significant agglomeration; as such, we lowered the level of surface ligand coverage and thus, the generation of a positive zeta potential for the amine-ligand functionalized CNCs was compromised. The zeta potential of the CNC-Carb was of lower magnitude than the CNC-Sulf, suggesting that the sulfated nanocrystals were

more resistant to compression of the double (stern and diffuse) layer by the salt ions in the fishwater medium.

For the cellulose nanofibers, TEMPO mediated chemical synthesis (CNF-T) had the most negative zeta potential (−41.1 ± 1.7 mV), whereas the mechanically homogenized samples (CNF-H and CNF-Maine) both had zeta potentials much closer to zero (−8.3 ± 1.1 and −10.1 ± 0.9, respectfully). These findings highlight the importance of understanding how the biological media surrounding a nanomaterial drives the net charge, which, in turn, impacts the fate and distribution of nanomaterials in biological systems (Bozich et al. 2014; Fubini et al. 2010; Lesniak et al. 2013).

CNC toxicity to embryonic zebrafish

The results from the embryonic zebrafish assay indicated that overall CNC materials, regardless of chemical modification, induced relatively low incidences of mortality or any other developmental impairment measured at concentrations below 1000 mg/L during the 5-day continuous exposure (Fig. 2). No significant sublethal impacts of CNC on developing zebrafish were found at 200 mg/L for any of the 19 sublethal impact endpoints assessed in this study. It should be noted that testing of surface ligand toxicity in the absence of CNC conjugation was not conducted, as ligand response alone is not necessarily representative of nanoparticle-biological interactions. In addition, many of the ligands had a lack of solubility in water in the absence of conjugation to CNC prohibiting testing with zebrafish.

Comparison of CNC materials functionalized with the amine-based ligands, N-ethylenediamine and N-hexamethylenediamine, which are structurally similar but have different ligand chain lengths, showed no differences in toxicity between the types of amine groups. Although both materials were synthesized using similar methodologies, CNC-Ethyl was synthesized from wood pulp and CNC-Hex was synthesized from cotton, thus the cellulose source seems to have little impact on the toxicity at our exposure concentrations (Fig. 2) nor the size of the synthesized CNC materials (Table 2). The amine-based ligands used in this study differ from those employed in other studies that have reported deleterious impacts of amine-based surface chemistry in other nanomaterial types (Hussain et al. 2009; Jones et al. 2012; Pryor et al. 2014; Schaeublin et al. 2011), suggesting that cellulose nanocrystals are uniquely low in toxicity or that amine ligand structure may impact biological responses to nanoparticles. The zeta potential measures of the crystals synthesized with amine-based ligands suggest only partial coverage of the surface with these ligands, thus it is not known to what extent the magnitude of cationic charge influences the uptake and/or toxicity of CNC materials. In addition, the agglomeration of materials was observed, particularly for the CNC-AEE, CNC_GMAC and CNC-Hex, which could have altered the bioavailability of the materials, and thus the degree of observed toxicity to the developing zebrafish.

Although the fiber-like shape and high surface to mass ratio allows for large surface loading of chemical ligands in nanocellulose materials, other types of fibrous nanomaterials, such as carbon nanotubes, have attributed observed toxicities to their high aspect ratio (Lanone et al. 2013). Similar to our results, other studies of fiber shaped nanomaterials, including metal or metal oxide rods or nanowires, wollastonite ($CaSiO_3$) and imogolite studies, have found that

the biological responses elicited by these nanomaterials seem to largely depend upon factors such as coating agent, impurities, defects, and agglomeration/aggregation state, rather than the fibrous structures themselves (Alkilany et al. 2009; Fubini et al. 2010; Gasser et al. 2012; Koyama et al. 2009; Liu et al. 2012; Maxim and McConnell 2005). Perhaps the high aspect ratio of CNC materials leads to steric or other hindrance at binding sites that impacts the uptake, distribution and/or metabolism of CNC. Overall, oxicological studies of CNC remain quite limited, especially across a diverse range of changes in surface chemistry. More studies with varied aspect ratio and variations in the number of surface ligands are warranted to support the continued development of cellulose nanomaterials.

CNF toxicity to embryonic zebrafish

The synthesis methods used to produce nanofibrillated materials rely on either chemical processes, mechanical processes, or some combination of both with each method introducing different physicochemical properties into the final cellulose material. Cellulose nanofiber (CNF) toxicity was evaluated for samples from the University of Maine Pilot Plant as well as two CNFs from the Forest Products Laboratory (Madison, WI) produced by either chemical synthesis (TEMPO method) or mechanical homogenization. Similar to the CNC results, overall CNF toxicity to developing zebrafish was low; however, mechanically homogenized CNFs from the Forest Products Laboratory displayed higher toxicity than similar fibers prepared using the TEMPO process, resulting in significant mortality at 250 mg/L (Fig. 3). Despite this finding, the University of Maine CNF, which was also prepared using mechanical homogenization, did not show any significant toxicity at 250 mg/L. Similar to the mortality data, significant sublethal impacts from CNF-H exposures included significant yolk sac and pericardial edema beginning at 250 mg/L, while none of the other sublethal endpoints occurred with any significance in this or the other two CNF samples (Fig. 4). The toxicity of CNF-H to zebrafish embryos, in the absence of CNF-Maine toxicity, suggests that the amorphous nanofibers with differential aspect ratios as a result of the mechanical homogenization methodology (Stelte and Sanadi 2009) or differences in the starting material may impact CNF toxicity. The indirect effect of differential aspect ratio impacts on agglomeration and in turn, available nanoparticle surface area, could also play a role in the observed patterns of toxicity (Eichhorn et al. 2010).

Significant impacts of synthesis methods on the biological responses elicitedintest organisms have been previously reported for other nanomaterials (Harper et al. 2014; Hussain et al. 2009; Schaeublin et al. 2011). Most toxicity studies have employed nano or micro cellulose materials synthesized by the common procedure of acid hydrolysis using sulfuric or hydrochloric acids (Clift et al. 2011; Kovacs et al. 2010; Male et al. 2012). CNC obtained from sulfuric acid hydrolysis disperses more readily in water due to the abundance of charged sulfate groups on its surface; however, its toxicity did not differ from carboxylated CNC. By comparing the chemical synthesis methods to mechanical synthesis methods we have determined that mechanical homogenization can, but does not always, result in increased toxicity of CNFs. Future studies comparing the toxicity of CNF produced by various mechanical methods are needed to elucidate the cause of differences observed in toxicity. Potential reasons for the difference in toxicity between mechanically processed

CNFs include the type of mechanical processing, the cellulose material source, end-product impurities related to purification methods and/or aspect ratio.

Uptake of fluorescent CNC

In order to rule out the potential that CNC is not bioavailable, we assessed the uptake of CNC by zebrafish during development using fluorescently labeled CNC. Toxicity tests with fluorescently tagged CNC showed that the toxicity was similar to the carboxylated (unlabeled) CNC, with no significant mortality or developmental abnormalities observed at the highest dose tested (2000 mg/L). Fluorescent microscopy images of embryos exposed to 100 or 500 mg/L Rhodamine labeled CNC indicated uptake of the labeled particles (measured as integrated density) over the first 3 days, and then a dramatic increase on day 4 and 5, possibly due to the onset of mouth gaping behavior resulting in ingestion (Fig. 5). The chorionic membrane overall did not statistically impact uptake during exposure. Considering a chorionic pore size of 0.5–0.7 lm, it is likely that the nanomaterials were still capable of entering the chorion and accessing the embryos (Lee et al. 2007).

Confocal microscopy of exposed embryos identified heavily concentrated locations within the embryos (Fig. 6). The similarities in the distribution of fluorescence to those reported by Whitfield, 1996 during histological staining of the lateral lines in similar aged zebrafish, suggest CNC distribution to the lateral line neuromasts of the integumentary system (Whitfield et al. 1996). Control embryos not exposed to fluorescently labeled CNC showed no change in fluorescence over the 5 days incubation period (Fig. 6). Embryos exposed to Rhodamine B fluorophore alone exhibited distinct differences in the distribution of fluorescence compared to Rhodamine B labeled nanocrystalline cellulose (Fig. 7), suggesting the fluorophore remained attached to the material and that localization was, to some extent, CNC mediated. These data suggest that fluorescent (carboxylated) CNC was taken up both dermally throughout the exposure and orally by the embryos at later stages of development when mouth gaping behavior initiates.

Conclusions

Studies determining the safety of cellulose nanomaterials are essential because their biointeractions are expected to occur at increasing frequencies given the increasing wide-spread use of these materials. The overall goal of the present study was to determine the toxicological profile of a series of cellulose-based nanomaterials following physicochemical modifications in order to identify design principles for creating products with minimal hazard.

We hypothesized that the aspect ratio and synthesis process for nanocellulose materials would influence their toxic potential, and that amine surface chemistry would drive the toxicity of CNC-surface modified materials. Our results indicate that CNCs and CNFs have overall low toxicity to developing zebrafish and that the high aspect ratio of CNCs and CNFs is not a predominant predictor of their toxic potential. Cellulose nanocrystals had an overall low potential for toxicity at relevant exposure concentrations. Surface chemical modifications did not significantly alter CNC toxicity to the extent reported for many other nanoparticle types with respect to changes in surface charge (Bonventre et al. 2014; Harper

et al. 2014; Pryor et al. 2014). In summary, nanocellulose materials can be used as a model platform to systematically investigate the inherent features driving nanomaterial toxicity. In doing so, we can take steps to protect workers, consumers and the environment from suspect nanocellulose materials and guide the development of safer materials in the future.

Acknowledgments

We want to thank BioVision Inc., NIOSH and University of Maine Process Development Center for supplying some of the cellulose materials. We would also like to thank the staff of Sinnhuber Aquatic Research Laboratory for providing the embryos and Mike Adamic and Kayla Guldager for assistance with the material synthesis and characterization. These studies were supported with funding from #ES017552-01A2; #P30ES03850; #ES0166896-01; #FA8650-05-1-15041; P30ES000210. This material is based upon work supported by the National Science Foundation via the Major Research Instrumentation (MRI) Program under Grant No. 1040588. We also gratefully acknowledge financial support for acquisition of the TEM instrument from Murdock Charitable Trust and the Oregon Nanoscience and Microtechnologies Institute (ONAMI). Mention of a specific product or company does not constitute endorsement by the Centers for Disease Control and Prevention. The findings and conclusions in this report are those of the authors and do not necessarily represent the views of NIOSH. The research at NIOSH/CDC was funded by the US National Toxicology Program under Inter-Agency Agreement #11-NS11-04-M01.

Abbreviations

hpf	Hours post-fertilization
CNC	Cellulose nanocrystals
CNF	Cellulose nanofibers
NP	Nanoparticle
TEMPO	2,2,6,6-Tetramethylpiperidine-1-oxyl radical
MCC	Microcrystalline cellulose
MFC	Micro-fibrillated cellulose
EDC	1-Ethyl-3-[3-dimethylaminopropyl] carbodiimide hydrochloride
AEE	2-,2-Aminoethoxyethanol
GMAC	Glycidyltrimethylammonium chloride
DI	Distilled water
RO	Reverse osmosis
RBF	Round bottom flask
NIOSH	National Institute for Occupational Safety and Health
MWCO	Molecular weight cut-off
ANOVA	Analysis of variance

References

Alexandrescu L, Syverud K, Gatti A, Chinga-Carrasco G. Cytotoxicity tests of cellulose nanofibril-based structures. Cellulose. 2013; 20:1765–1775.

Alkilany AM, Nagaria PK, Hexel CR, Shaw TJ, Murphy CJ, Wyatt MD. Cellular uptake and cytotoxicity of gold nanorods: molecular origin of cytotoxicity and surface effects. Small. 2009; 5:701–708. [PubMed: 19226599]

Azizi Samir MAS, Alloin F, Dufresne A. Review of recent research into cellulosic whiskers, their properties and their application in nanocomposite field. Biomacromolecules. 2005; 6:612–626. [PubMed: 15762621]

Bonventre J, Pryor J, Harper B, Harper S. The impact of aminated surface ligands and silica shells on the stability, uptake, and toxicity of engineered silver nanoparticles. J Nanopart Res. 2014; 16:1–15.

Bozich JS, Lohse SE, Torelli MD, Murphy CJ, Hamers RJ, Klaper RD. Surface chemistry, charge and ligand type impact the toxicity of gold nanoparticles to *Daphnia magna*. Environ Sci Nano. 2014; 1:260–270.

Brinchi L, Cotana F, Fortunati E, Kenny J. Production of nanocrystalline cellulose from lignocellulosic biomass: technology and applications. Carbohydr Polym. 2013; 94:154–169. [PubMed: 23544524]

Clift MJ, et al. Investigating the interaction of cellulose nanofibers derived from cotton with a sophisticated 3D human lung cell coculture. Biomacromolecules. 2011; 12:3666–3673. [PubMed: 21846085]

Dufresne A. Nanocellulose: a new ageless bionanomaterial. Mater Today. 2013; 16:220–227.

Eichhorn S, et al. Review: current international research into cellulose nanofibres and nanocomposites. J Mater Sci. 2010; 45:1–33.

Elazzouzi-Hafraoui S, Nishiyama Y, Putaux J-L, Heux L, Dubreuil F, Rochas C. The shape and size distribution of crystalline nanoparticles prepared by acid hydrolysis of native cellulose. Biomacromolecules. 2007; 9:57–65. [PubMed: 18052127]

Fubini B, Ghiazza M, Fenoglio I. Physico-chemical features of engineered nanoparticles relevant to their toxicity. Nanotoxicology. 2010; 4:347–363. [PubMed: 20858045]

Gasser M, et al. Pulmonary surfactant coating of multi-walled carbon nanotubes (MWCNTs) influences their oxidative and pro-inflammatory potential in vitro. Part Fibre Toxicol. 2012; 9:17. [PubMed: 22624622]

Goussé C, Chanzy H, Excoffier G, Soubeyrand L, Fleury E. Stable suspensions of partially silylated cellulose whiskers dispersed in organic solvents. Polymer. 2002; 43:2645–2651.

Hanif Z, Ahmed FR, Shin SW, Kim Y-K, Um SH. Size-and dose-dependent toxicity of cellulose nanocrystals (CNC) on human fibroblasts and colon adenocarcinoma. Coll Surf B Biointerfaces. 2014; 119:162–165.

Harper B, Sinche F, Ho Wu R, Gowrishankar M, Marquart G, Mackiewicz M, Harper S. The impact of surface ligands and synthesis method on the toxicity of glutathione-coated gold nanoparticles. Nanomaterials. 2014; 4:355–371. [PubMed: 26213631]

Hasani M, Cranston ED, Westman G, Gray DG. Cationic surface functionalization of cellulose nanocrystals. Soft Matter. 2008; 4:2238–2244.

Hemraz UD, Boluk Y, Sunasee R. Amine-decorated nanocrystalline cellulose surfaces: synthesis, characterization, and surface properties. Can J Chem. 2013; 91:974–981.

Hua K, Carlsson DO, Ålander E, Lindström T, Strømme M, Mihranyan A, Ferraz N. Translational study between structure and biological response of nanocellulose from wood and green algae. RSC Adv. 2014; 4:2892–2903.

Hussain SM, et al. Toxicity evaluation for safe use of nanomaterials: recent achievements and technical challenges. Adv Mater. 2009; 21:1549–1559.

Isogai A, Saito T, Fukuzumi H. TEMPO-oxidized cellulose nanofibers. Nanoscale. 2011; 3:71–85. [PubMed: 20957280]

Jackson JK, Letchford K, Wasserman BZ, Ye L, Hamad WY, Burt HM. The use of nanocrystalline cellulose for the binding and controlled release of drugs. Int J Nanomed. 2011; 6:321–330.

Jones CF, et al. Cationic PAMAM dendrimers aggressively initiate blood clot formation. ACS Nano. 2012; 6:9900–9910. [PubMed: 23062017]

Kovacs T, et al. An ecotoxicological characterization of nanocrystalline cellulose (NCC). Nanotoxicology. 2010; 4:255–270. [PubMed: 20795908]

Koyama S, et al. In vivo immunological toxicity in mice of carbon nanotubes with impurities. Carbon. 2009; 47:1365–1372.

Lam E, Hrapovic S, Majid E, Chong JH, Luong JHT. Catalysis using gold nanoparticles decorated on nanocrystalline cellulose. Nanoscale. 2012a; 4:997–1002. [PubMed: 22218753]

Lam E, Male KB, Chong JH, Leung ACW, Luong JHT. Applications of functionalized and nanoparticle-modified nanocrystalline cellulose. Trends Biotechnol. 2012b; 30:283–290. [PubMed: 22405283]

Lanone S, Andujar P, Kermanizadeh A, Boczkowski J. Determinants of carbon nanotube toxicity. Adv Drug Deliv Rev. 2013; 65:2063–2069. [PubMed: 23928473]

Lasseuguette E. Grafting onto microfibrils of native cellulose. Cellulose. 2008; 15:571–580.

Lee KJ, Nallathamby PD, Browning LM, Osgood CJ, Xu X-HN. In vivo imaging of transport and biocompatibility of single silver nanoparticles in early development of zebra-fish embryos. ACS Nano. 2007; 1:133–143. [PubMed: 19122772]

Lesniak A, Salvati A, Santos-Martinez MJ, Radomski MW, Dawson KA, Åberg C. Nanoparticle adhesion to the cell membrane and its effect on nanoparticle uptake efficiency. J Am Chem Soc. 2013; 135:1438–1444. [PubMed: 23301582]

Liu W, et al. Influence of the length of imogolite-like nanotubes on their cytotoxicity and genotoxicity toward human dermal cells. Chem Res Toxicol. 2012; 25:2513–2522. [PubMed: 22989002]

Male KB, Leung AC, Montes J, Kamen A, Luong JH. Probing inhibitory effects of nanocrystalline cellulose: inhibition versus surface charge. Nanoscale. 2012; 4:1373–1379. [PubMed: 22252333]

Maxim LD, McConnell E. A review of the toxicology and epidemiology of wollastonite. Inhal Toxicol. 2005; 17:451–466. [PubMed: 16020040]

Moon RJ, Martini A, Nairn J, Simonsen J, Youngblood J. Cellulose nanomaterials review: structure, properties and nanocomposites. Chem Soc Rev. 2011; 40:3941–3994. [PubMed: 21566801]

Morandi G, Heath L, Thielemans W. Cellulose nanocrystals grafted with polystyrene chains through surface-initiated atom transfer radical polymerization (SI-ATRP). Langmuir. 2009; 25:8280–8286. [PubMed: 19348498]

Müller A, Wesarg F, Hessler N, Müller FA, Kralisch D, Fischer D. Loading of bacterial nanocellulose hydrogels with proteins using a high-speed technique. Carbohydr Polym. 2014; 106:410–413. [PubMed: 24721096]

Peng B, Dhar N, Liu H, Tam K. Chemistry and applications of nanocrystalline cellulose and its derivatives: a nanotechnology perspective. Can J Chem Eng. 2011; 89:1191–1206.

Pryor JB, Harper BJ, Harper SL. Comparative toxicological assessment of PAMAM and thiophosphoryl dendrimers using embryonic zebrafish. Int J Nanomed. 2014; 9:1947.

Riddick, T. Control of colloid stability through zeta potential: with a closing chapter on its relationship to cardiovascular disease. Vol. 1. Wynnewood: Livingston Publishing Company; 1968.

Roman M. Toxicity of cellulose nanocrystals: a review. Ind Biotechnol. 2015; 11:25–33.

Schaeublin NM, Braydich-Stolle LK, Schrand AM, Miller JM, Hutchison J, Schlager JJ, Hussain SM. Surface charge of gold nanoparticles mediates mechanism of toxicity. Nanoscale. 2011; 3:410–420. [PubMed: 21229159]

Sharifi S, Behzadi S, Laurent S, Forrest ML, Stroeve P, Mahmoudi M. Toxicity of nanomaterials. Chem Soc Rev. 2012; 41:2323–2343. [PubMed: 22170510]

Siqueira G, Tapin-Lingua S, Bras J, da Silva Perez D, Dufresne A. Morphological investigation of nanoparticles obtained from combined mechanical shearing, and enzymatic and acid hydrolysis of sisal fibers. Cellulose. 2010; 17:1147–1158.

Stelte W, Sanadi AR. Preparation and characterization of cellulose nanofibers from two commercial hardwood and softwood pulps. Ind Eng Chem. 2009; 48:11211–11219.

Truong, L.; Harper, S.; Tanguay, R. Evaluation of embryotoxicity using the zebrafish model. In: Gautier, J-C., editor. Drug safety evaluation: methods in molecular biology. Vol. 691. New York: Humana Press; 2011. p. 271-279.

Turbak AF, Snyder FW, Sandberg KR. Microfibrillated cellulose, a new cellulose product: properties, uses, and commercial potential. J Appl Polym Sci. 1983; 37:815–827.

Usenko CY, Harper SL, Tanguay RL. Fullerene C60 exposure elicits an oxidative stress response in embryonic zebrafish. Toxicol Appl Pharmacol. 2008; 229:44–55. [PubMed: 18299140]

Whitfield TT, et al. Mutations affecting development of the zebrafish inner ear and lateral line. Development. 1996; 123:241–254. [PubMed: 9007244]

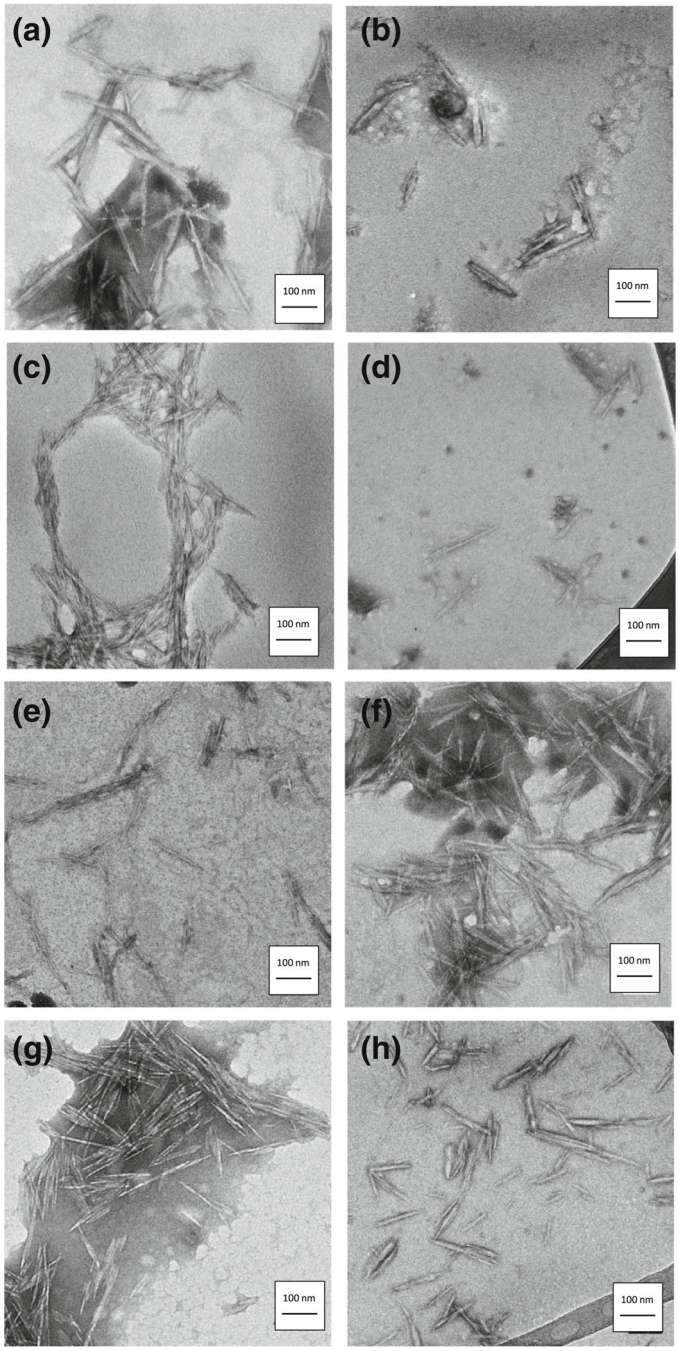

Fig. 1.

Representative TEM images of nanocellulose materials TEM images with scale bar for nanocellulose materials including **a** carboxylated (CNC-Carb), **b** taurine modified (CNC-Taur), **c** sulfated (CNC-Sulf), **d** ethoxyethanol modified (CNC-AEE), **e** hexamethylenediamine modified (CNC-Hex), **f** ethylenediamine modified (CNC-Ethyl), **g** GMAC modified (CNC-GMAC) and **h** Rhodamine B tagged (CNC-Rhod) nanocrystals

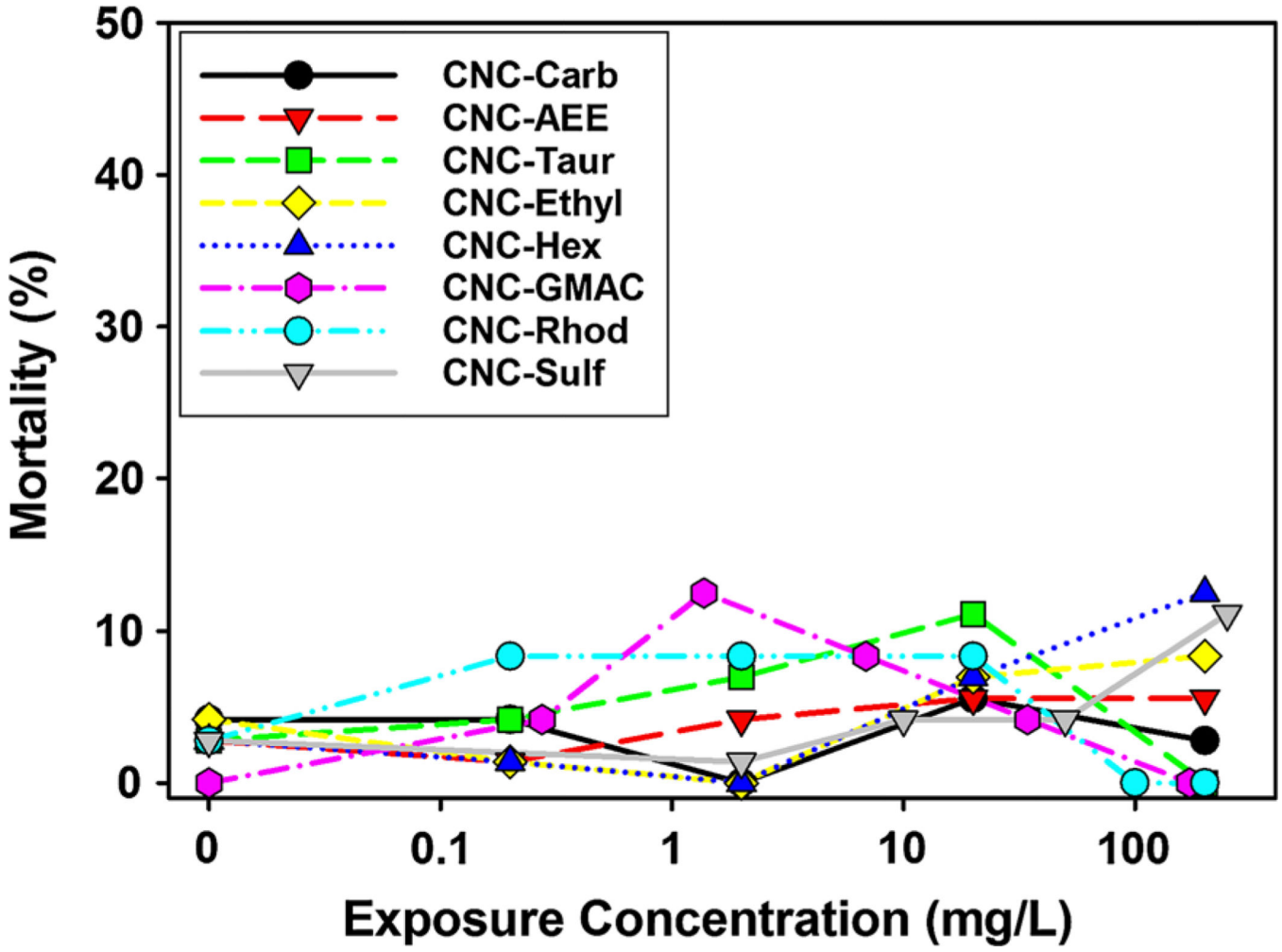

Fig. 2.

Mortality rate for CNC exposed embryonic zebrafish Percent mortality of embryos (n = 24 at each exposure concentration) exposed to increasing concentrations of cellulose nanocrystals (CNC) with varying surface chemistry and charge. *Asterisk* indicates significant difference ($p \leq 0.05$) from control (fishwater alone)

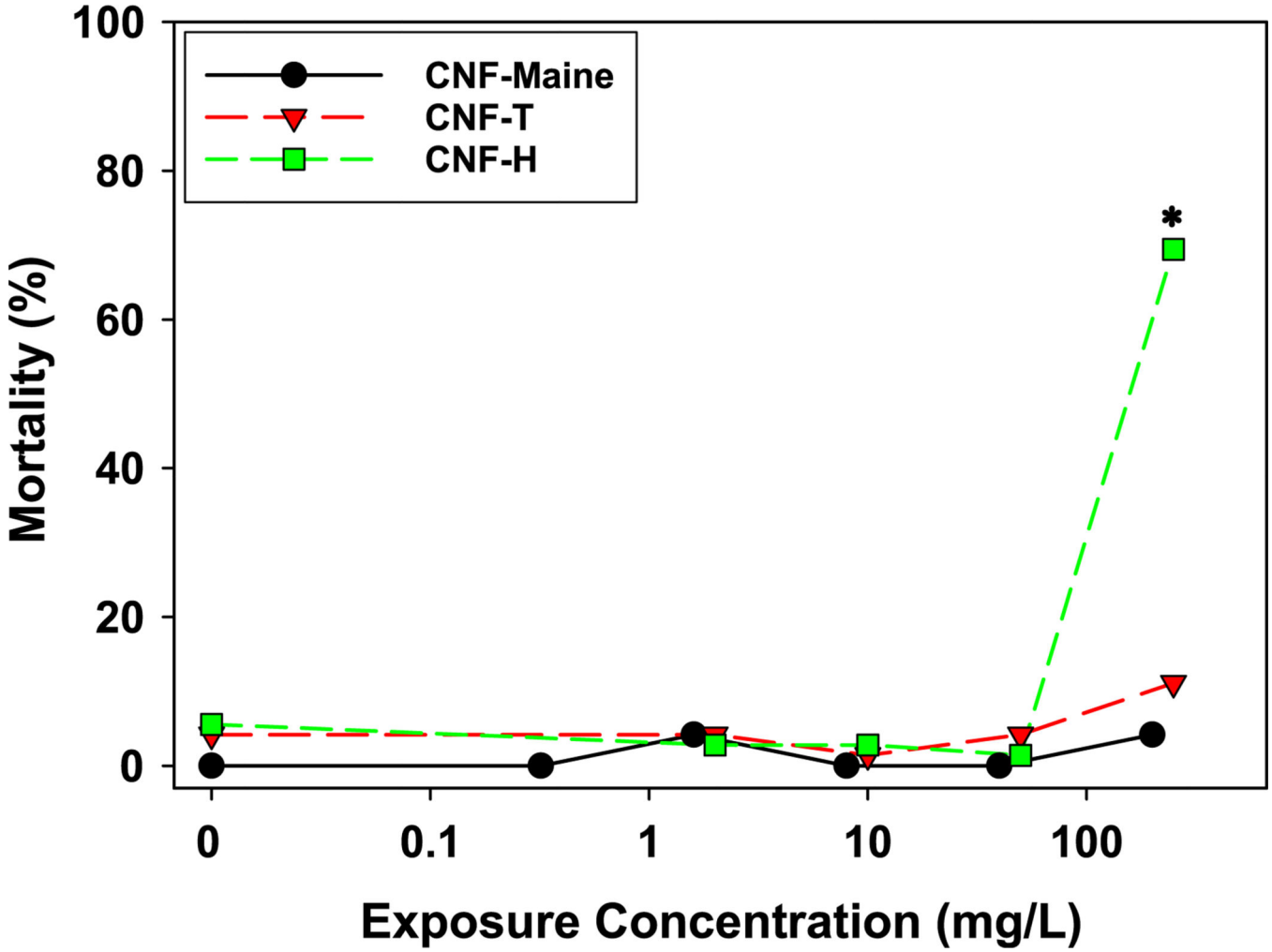

Fig. 3.

Mortality rate for CNF exposed embryonic zebrafish Percent mortality for embryonic zebrafish (n = 24 at each exposure concentration) exposed to increasing concentrations of cellulose nanofibers (CNF). *Asterisk* indicates significant difference ($p \leq 0.05$) from control (fishwater alone)

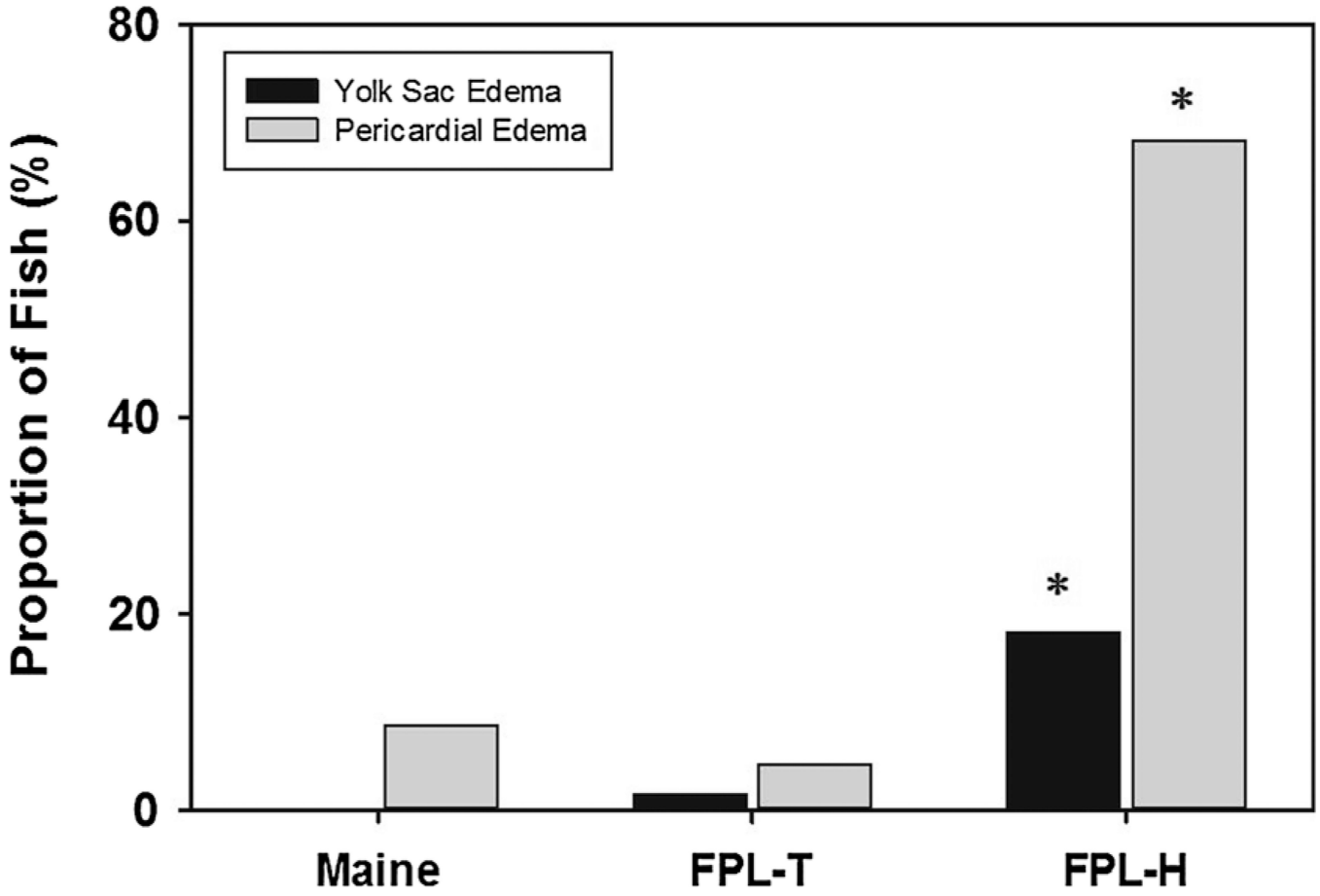

Fig. 4.

Sub-lethal impacts on developing zebrafish Incidence rate of pericardial and yolk sac edema in developing zebrafish exposed to 250 mg/L of chemically (CNF-T) and mechanically (CNF-H, Maine) synthesized cellulose nanofibers (CNF) during the first 5 days of development. *Asterisk* indicates significant difference ($p \leq 0.05$) from control embryos (no exposure to CNFs)

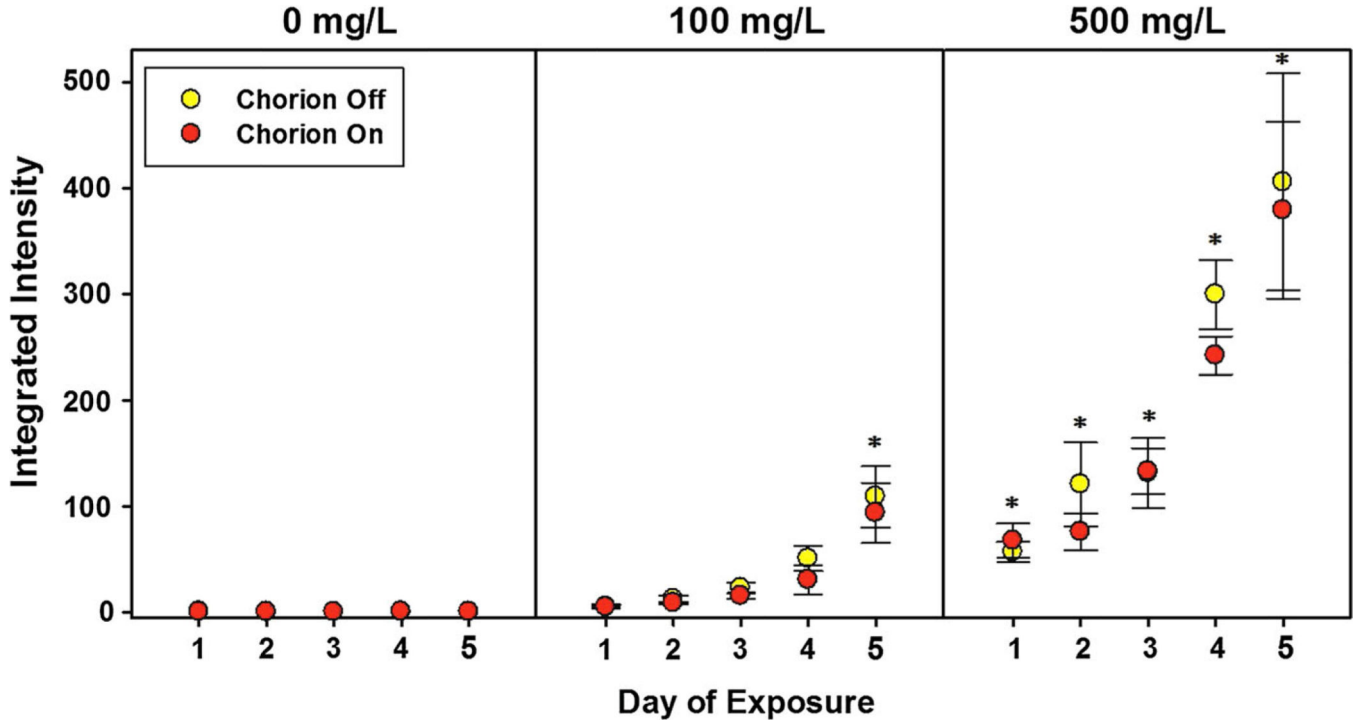

Fig. 5.

Uptake of Rhodamine-labeled CNC by developing zebrafish Uptake of Rhodamine labeled cellulose nanocrystals following fluorescent imaging (with chorionic membrane present or absent) from 8 to 120 h post-fertilization in developing zebrafish. *Asterisk* indicate significant increases in intensity from control exposure ($p \leq 0.05$, n = 6 embryos)

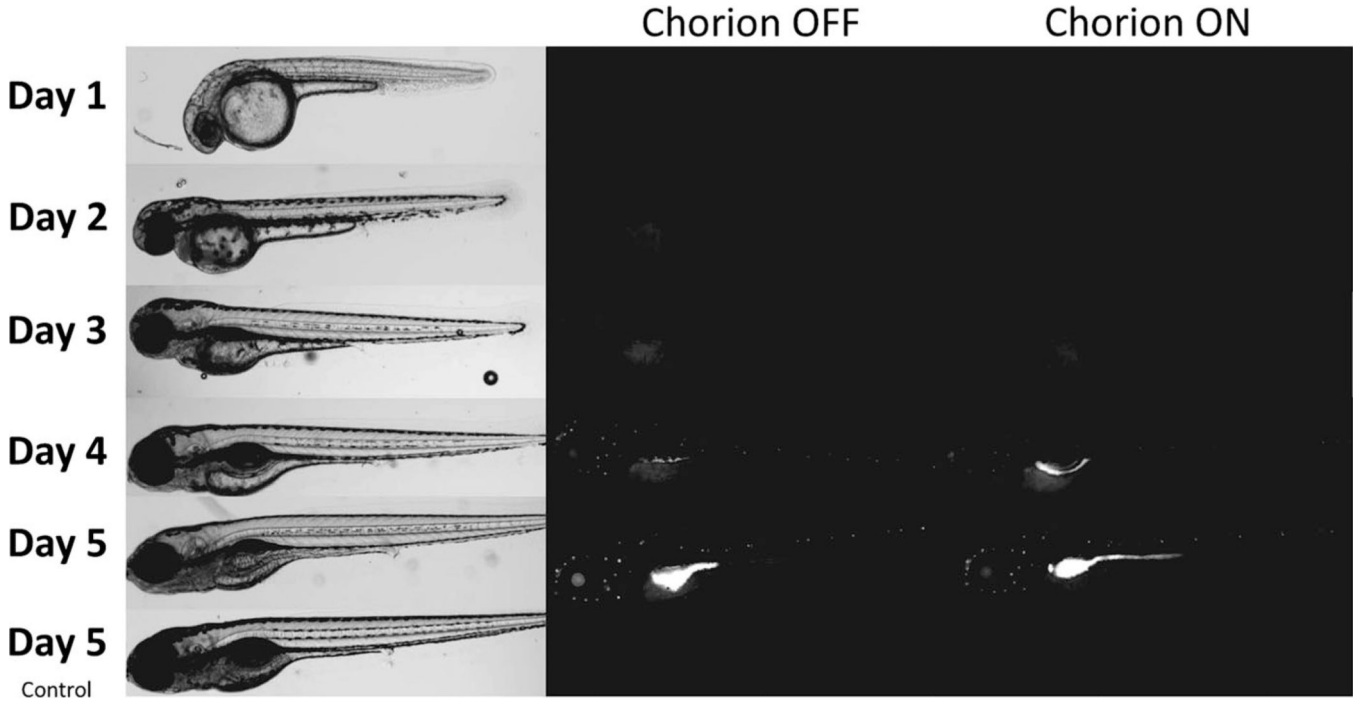

Fig. 6.

Fluorescence images of developing embryos exposed to Rhodamine labeled CNC Representative images of 1–5 day old zebrafish following continuous exposure to 500 mg/L Rhodamine B labeled CNC beginning at 8 hpf. *Left panel* shows bright-field microscopic images and the *right panel* shows measured fluorescence intensity

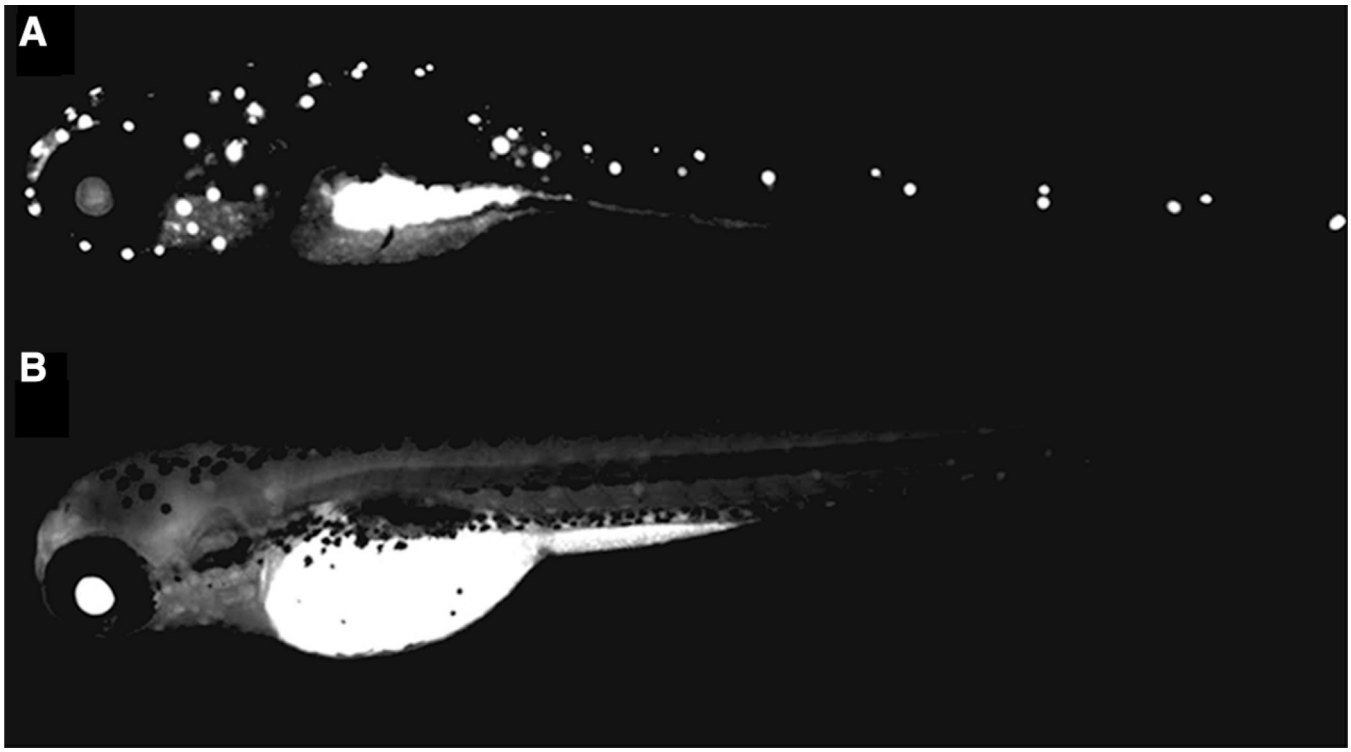

Fig. 7.

Comparison of embryo fluorescence with Rhodamine alone or conjugated to CNC

Representative images of zebrafish embryos at 4 days post-fertilization exposed to **a** 500 mg/L Rhodamine B tagged CNC and **b** 1 mg/L Rhodamine B fluorophore alone

Table 1

Description of the various surface chemistries investigated, the surface charge of each ligand and the source of the cellulose used for synthesis

Material	Surface chemical modification	Surface ligand charge	Cellulose source material
CNC-Carb	Carboxylated	Anionic	Wood Pulp
CNC-Taur	Taurine	Anionic	Cotton
CNC-Sulf	Sulfated	Anionic	Kraft Pulp
CNC-AEE	Ethoxyethanol	Neutral	Cotton
CNC-Hex	Hexamethylenediamine	Neutral	Cotton
CNC-Ethyl	Ethylenediamine	Neutral	Wood Pulp
CNC-GMAC	Glycidyltrimethylammonium chloride	Cationic	Cotton
CNC-Rhod	Rhodamine B	Cationic	Cotton
CNF-FPL-T[a]	Carboxylated	Anionic	Kraft Pulp
CNF-FPL-H[b]	None	–	Kraft Pulp
CNF-Maine[c]	None	–	Wood Pulp

[a] Synthesized by forest products laboratory via TEMPO-oxidation

[b] Synthesized by forest products laboratory via mechanical homogenization

[c] Manufactured by University of Maine Pilot Plant by mechanical homogenization

Table 2

Physicochemical characteristics and zeta (ζ) potential (mean ± SD) of CNC materials in exposure media (fishwater)

Material	Length (nm)	Width (nm)	Zeta (ζ) potential (mV)
CNC-Carb	137 ± 39	15 ± 2	−28.3 ± 0.4
CNC-Taur	124 ± 58	10 ± 4	−28.2 ± 0.2
CNC-Sulf	107 ± 79	5 ± 3	−38.0 ± 0.5
CNC-AEE	110 ± 63	10 ± 7	−26.9 ± 0.5
CNC-Hex	129 ± 63	9 ± 3	−29.0 ± 0.3
CNC-Ethyl	123 ± 48	9 ± 3	−17.7 ± 2.6
CNC-GMAC	102 ± 44	6 ± 2	+5.1 ± 0.1
CNC-Rhod	125 ± 61	11 ± 4	−27.8 ± 5.6